Development of a wireless intra-ocular pressure monitoring system for incorporation into a therapeutic glaucoma drainage implant

Tarun Kakaday *[a], Malcolm Plunkett [c], Steven McInnes [b], Jim S. Jimmy Li [a], Nicolas H. Voelcker [b], and Jamie E. Craig [d]

[a] School of Computer Science, Engineering & Mathematics, Flinders University, Adelaide, Australia
[b] School of Chemistry, Physics and Earth Sciences, Flinders University, Adelaide, Australia
[c] Ellex Medical Lasers R & D, 82 Gilbert Street, Adelaide, Australia
[d] Department of Ophthalmology, Flinders Medical Centre, Adelaide, Australia

ABSTRACT

Glaucoma is a common cause of blindness. Wireless, continuous monitoring of intraocular pressure (IOP) is an important, unsolved goal in managing glaucoma. An IOP monitoring system incorporated into a glaucoma drainage implant (GDI) overcomes the design complexity associated with incorporating a similar system in a more confined space within the eye. The device consists of a micro-electro-mechanical systems (MEMS) based capacitive pressure sensor integrated with an inductor printed directly onto a polyimide printed circuit board (PCB). The device is designed to be incorporated onto the external plate of a therapeutic GDI. The resonance frequency changes as a function of IOP, and is tracked remotely using a spectrum analyzer. A theoretical model for the reader antenna was developed to enable maximal inductive coupling with the IOP sensor implant. Pressure chamber tests indicate that the sensor implant has adequate sensitivity in the IOP range with excellent reproducibility over time. Additionally, we show that sensor sensitivity does not change significantly after encapsulation with polydimethylsiloxane (PDMS) to protect the device from fluid environment. *In vitro* experiments showed that the signal measured wirelessly through sheep corneal and scleral tissue was adequate indicating potential for using the system in human subjects.

Keywords: Glaucoma, intraocular pressure (IOP), glaucoma drainage implant (GDI), micro-electro-mechanical systems (MEMS), capacitive pressure sensors, reader antenna, printed circuit boards (PCB's).

1. INTRODUCTION

Glaucoma is a heterogeneous disease characterized by pathological retinal nerve fiber layer loss which if left untreated culminates in blindness. The major identified risk factor in glaucoma is elevated intraocular pressure (IOP), and despite some patients not having an IOP elevated above the normal population range, the only proven therapeutic intervention is IOP reduction. All current treatments, whether medical or surgical, primarily act by lowering IOP. Thus, the accurate monitoring of IOP is an essential clinical facet in glaucoma care.

Currently, there are a wide range of modalities available for routine IOP measurement. The most commonly used technique, and current gold standard is applanation tonometry, where the tonometer head directly applanates the cornea. The force required to achieve a fixed degree of applanation provides an approximation of the pressure within the eye resisting this deformation. In addition to requiring topical anesthetic and a skilled operator, a major disadvantage of applanation tonometry is that it is influenced by many variables, thereby providing only a surrogate measure of true IOP. Additionally, diurnal measurements are difficult to obtain, particularly overnight. Remote continuous monitoring of IOP has been long desired by clinicians and the development of such technology has the potential of revolutionizing glaucoma care by enabling remote monitoring.

*kaka0005@flinders.edu.au; mobile: +618412914380

To allow long term and real time monitoring of IOP, a fully implantable telemetric pressure sensing system is required. One approach to this is an inductor-capacitor resonant circuit formed by a capacitive sensor with adequate sensitivity in the IOP range (5 - 50 mmHg) in parallel with an inductor coil. The inductor coil acts both as an inductance and as an antenna. The IOP sets the capacitance, and thus the resonant frequency of the circuit. By remotely sensing the resonant frequency, the pressure can be measured.

Several groups have described an active remote measuring device that can be incorporated into the haptic region of an intraocular lens (IOL). IOL's are universally used to replace the opaque natural lens in cataract surgery, given the large demand for cataract surgery and the usual marked gain in visual function resulting from the procedure, the coupling of an IOP sensor with an IOL implant is an attractive prospect.[1-3]The IOL is in direct contact with the aqueous humor inside the anterior chamber providing an accurate measurement of IOP. However, the IOL has size and weight constraints requiring the sensor and inductor to be heavily miniaturized and therefore requiring on-chip circuitry to amplify and process signals (i.e. active telemetry). Whilst active devices are accurate and sensitive, their complexity and manufacturing price are potentially major obstacles to a wide spread use.

In another approach, Leonardi et al. [4] describes an indirect method in which a micro strain gauge is embedded into a soft contact lens that measures changes in corneal curvature correlated to IOP. The authors claim that the micro strain gauge is adequately sensitive and tracks the IOP variations well. However, the correlation between corneal curvature and IOP is not universally accepted [5]. The changes in corneal curvature are extremely small and of poor reproducibility.

A glaucoma drainage implant (GDI) is a device implanted to enable lowering of IOP in severe glaucoma cases. The explant plate of a GDI which is implanted under the conjunctiva is directly connected to the anterior chamber of the eye via a tube. The plate provides a larger surface area (135 mm^2 in a single plate Molteno GDI) compared to an IOL allowing greater flexibility in design for a larger antenna coil and capacitive pressure sensor to be incorporated. A passive telemetry approach is suitable in such a case. This reduces the fabrication complexity making the device low cost and simple to fabricate. In addition, there are no active parts in the system making it desirable for implantation.

It is not certain if the pressure measured at the explant plate of the GDI is an accurate estimate of the true IOP. This paper therefore investigates the feasibility and implementation of an IOP monitoring device in a GDI. This paper also investigates the optimal design of the reader antenna to maximize coupling between the sensor implant and external interrogating device (i.e. the spectrum analyzer). Whilst this paper focuses on the Molteno GDI, our methodology can be adapted to other GDI's available on the market.
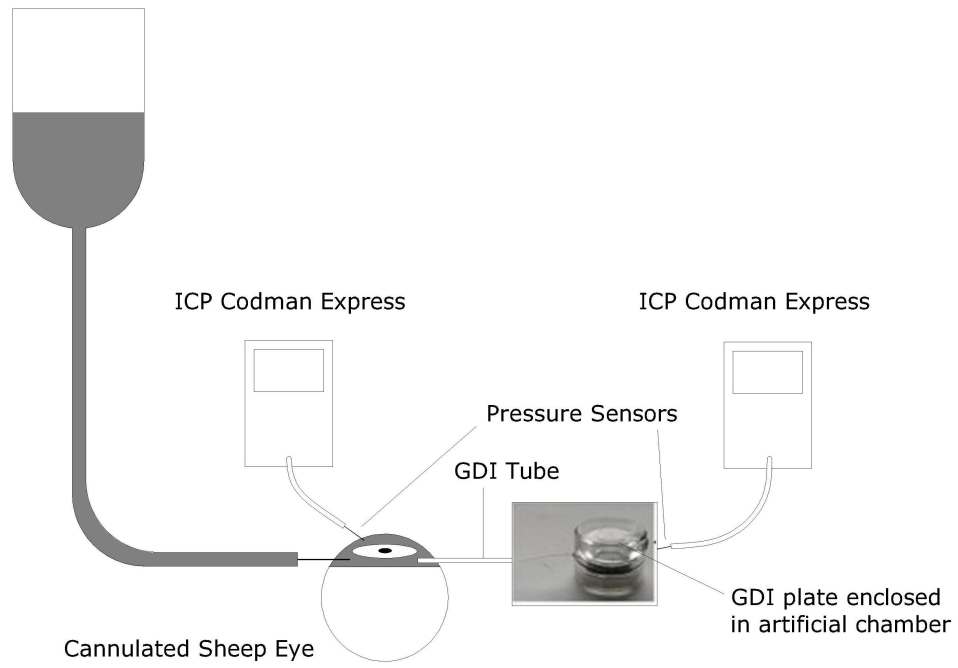
2. THEORETICAL BACKGROUND

2.1 Detection principle

The 'grid dip' principle is employed to detect the resonance frequency of the sensor implant. The sensor implant design consists of the capacitive pressure sensor (C) coupled in parallel with an inductor (L) to form a resonant circuit. The change in capacitance due to the change in IOP is correlated with resonance frequency (f) given by the expression

$$f = \frac{1}{2\pi\sqrt{LC}} \tag{1}$$

The voltage controlled oscillator (VCO) inside the spectrum analyzer sweeps though a specified range of frequencies, and when the sensor implant is brought near the vicinity of the external reader antenna connected to the spectrum analyzer a portion of the RF energy is absorbed by the sensor implant.[6] The amount of power absorbed is highest at its resonance frequency, corresponding to a 'dip' in the spectrum. The change in resonance frequency due to the changes in sensor capacitance can be tracked by observing the shift in the 'dip'. This method to remotely monitor resonance frequency changes due to change in pressure was successfully implemented, the design of the sensor implant and reader antenna are presented in the rest of this paper.
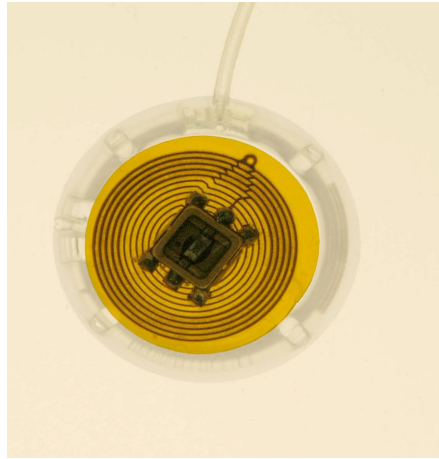
ICP Codman Express

ICP Codman Express

Pressure Sensors

GDI Tube

Cannulated Sheep Eye

GDI plate enclosed
in artificial chamber

Figure 2: The IOP sensor implant adhesively placed onto the explant plate of a Molteno GDI.

Table 1. Sensor inductor coil properties

Diameter (mm)	9.398
Track Width (μm)	127
Track Spacing (μm)	127
Track Thickness (μm)	70
Number of turns	18
Inductance (μH)	2.90
SRF (MHz)	63
D.C Resistance (Ω)	1.6

The sensor inductor was characterized using a Vector Impedance Meter (VIM) (Model 4815A Hewlett Packard -USA), and the obtained properties are listed in Table 1. It is highly desired that the resonance frequency of the sensor implant be well below the self resonating frequency (SRF) of the sensor inductor.

3.3 Capacitive sensor

The capacitive pressure sensors (E1.3N) (Microfab Bremen – Germany) measure the absolute pressure with a pressure range between 375mmHg - 975 mmHg, falling well within the IOP range (~760 mmHg – 800 mmHg incorporating atmospheric pressure). The capacitive sensors operate in both normal and touch mode.

To determine sensor sensitivity, the MEMS based capacitive sensors were soldered onto the inside of a pressure chamber I (Engineering workshop, Flinders University) connected to a programmable RLC meter (PM 6304, Philips) and a sphygmomanometer (Testo 510). The pressure inside the chamber was varied in the IOP range using an inflation cuff and the capacitance change was monitored though the RLC meter. The quality factor (Q) of the MEMS based capacitive pressure sensor was determined at the frequencies of interest using the VIM.

3.4 Wireless communication

Wireless communication between the sensor implant and external reader antenna is an important consideration for implantable systems since the RF has to penetrate though biological tissue. The wireless communication was evaluated by placing the sensor implant inside a pressure chamber II (Engineering workshop, Flinders University) connected to an

inflation cuff at one end and a sphygmomanometer (Testo 510) at the other. The sensor implant is separated from the reader antenna by a 4 mm thick PDMS barrier. The pressure was varied in the desired IOP range using the inflation cuff and the shift in the resonance peak as seen on the spectrum analyzer is recorded. Experiments were repeated replacing the PDMS barrier with explanted sheep scleral and corneal tissue to determine if wireless communication was possible through biological tissue.

3.5 Bio-coating

Polydimethylsiloxane (PDMS) is a widely used silicon-based polymer that is considered to be inert, non-toxic and non-flammable. All PDMS coatings were prepared from a two-component Sylgard® Brand 184 Silicone Elastomere Kit (Dow Corning – USA). The two components were mixed to give a transparent viscous elastomere which was degassed under vacuum before pouring an excess of the elastomere onto the sensor implant requiring coating. A thin film of PDMS was generated by spinning for 30 seconds at 3000 rpm using a spin coater. The PDMS was then cured in the oven at 80° C for a minimum of 1 hour.

3.6 Reader antenna design

Reader antenna design involves maximizing its read range by optimizing its inductive coupling with the sensor implant. The coupling coefficient k is given by the following expression [8,9]

$$k = \frac{M}{L_1 L_2} \tag{2}$$

where, M is the mutual inductance, L_1 and L_2 are the inductance of sensor and reader coils respectively. In applications, in order to obtain the best system characteristics, the value of k should be designed for unity. However there are several considerations that limit optimal coupling such as the size of sensor inductor which is in this case is limited by the size of the Molteno GDI and the SRF of the inductor coil, which should not interfere with the resonant frequency of the sensor implant The inductances L_1 and L_2 can be directly determined from the VIM and M is calculated by the solution provided by Zierhofer et al. [10].

$$M(a,b,\rho = 0, d) = \mu_o \sqrt{ab}\left[\left(\frac{2}{k} - k\right)K(k) - \frac{2}{k}E(k)\right]$$

where $\hspace{8cm}$ (3)

$$k \equiv \left(\frac{4ah}{(a+b)^2 + d^2}\right)^{1/2}$$

K (k) and E (k) are the complete elliptic integrals of the first and second kind, respectively. For multiple turns in the reader and sensor antenna the mutual inductance for a planar antenna becomes[10].

$$M_{ab} = \sum_{i=1}^{N_a}\sum_{j=1}^{N_b} M(a_i \cdot b_j \cdot \rho \cdot d) \tag{4}$$

In order to determine the optimal size for the reader antenna the mutual inductance between the two spiral coil geometries given by the expression below needs to maximized at a particular distance.[11]

$$M = \frac{\mu_o \pi N_1 N_2 (ab)^2}{2(a^2 + r^2)^{3/2}} \tag{5}$$

Where a, b are the radius of the reader and sensor coils respectively. N_1, N_2 are the number of turns in reader and sensor coil respectively, 'r' is the distance between the two coils. The above equation can be reduced to give:

$$a = \sqrt{2}r \tag{6}$$

The result indicates that that the optimum loop radius, a, is 1.414 times the demanded read range r.

4. RESULTS AND DISCUSSION

4.1 Feasibility study to incorporate a IOP monitoring system in an GDI

The pressure in an explanted sheep eye was varied from 5 mmHg - 50 mmHg by adjusting the height of a saline infusion bottle and the pressure in the artificial chamber of the GDI was simultaneously observed. The experiments were repeated at aqueous flow rates of 2 μl/min and 10 μl/min respectively. It was observed that the pressure in the anterior chamber of the cadaver sheep eye followed closely the pressure change in the artificial chamber with negligible delay. The results demonstrate that the pressure measured at the explant plate of the GDI is a good estimate of the true IOP inside the anterior chamber under physiological aqueous flow rates. The results are not unexpected as these experiments are to a certain extent subject to Poiseuille's Law

$$F = \frac{\Delta \mathrm{P} \mathrm{r}^4}{\frac{8}{\pi}\eta l} \tag{7}$$

Where the volumetric flow rate (F, meter³.second) is given by the pressure difference (ΔP, Pascal) divided by the viscosity (η) and the length (l, meters) and inversely proportional to the fourth power of the radius (r, meters). Substituting the Molteno GDI tube dimensions into (5) we get a negligible pressure drop of 0.01 mmHg – 0.10 mmHg at physiological flow rates of $1 - 10$ μl/min. From Poiseuille's Law it can be shown that the pressure difference between one end of the tube inserted into the anterior chamber and the other end of the tube is negligible.

4.2 Sensitivity of the sensor implant in the IOP range

The average sensitivity of the E1.3N capacitive pressure sensor in the IOP range was determined to be 1.20×10^{-3} pF/mmHg. The sensitivity analysis results showed that the capacitive sensors produced a detectable capacitance change for a pressure change between 8.2 mmHg - 10.4 mmHg across all data. VIM results as shown in Figure 3 reveal that the quality factor (Q) of the capacitive pressure sensor begins to drop with increasing frequency. The resonance frequency of the sensor implant is determined to be 38.61 MHz. The Q at the resonant frequency of the sensor implant is 8.71 as compared to the maximum Q of 57.29.
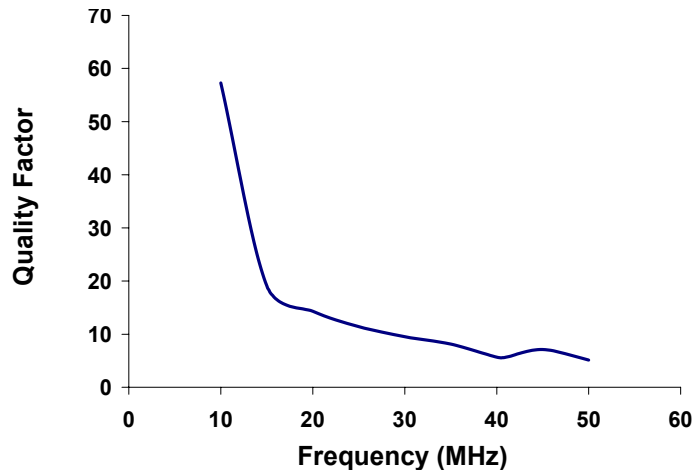
Figure 3: Quality factor of the MEMS capacitive pressure sensor relative to frequency.

Pressure chamber tests were randomly repeated (50 iterations) over a period of one week. The results are shown in Figure 4. The current resolution of the sensor implant in the IOP range is 10 mmHg. The resolution of the current system is limited by the sensitivity and Q of the MEMS capacitive sensor.
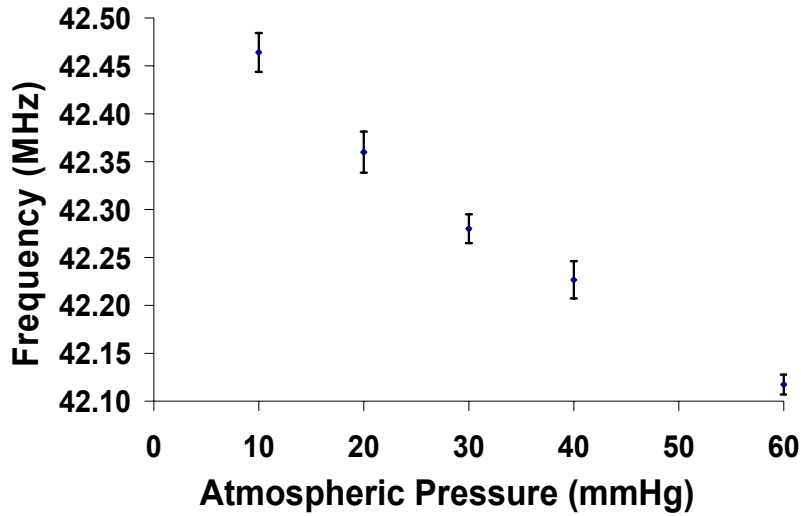
Figure 4: The resonance frequency response of the IOP sensor implant. The error bars indicate the standard deviation across 50 replicates.

In vitro experiments were carried out by substituting the 4mm PDMS barrier with explanted sheep corneal and scleral tissue. The results showed that the signal measured though ocular tissue in aqueous environment was adequate, indicating potential for using such a system in human subjects.

4.3 Encapsulation of sensor with PDMS

The MEMS based capacitive pressure sensors was encapsulated in PDMS in order to prevent exposure of the sensor to aqueous environment. In order to determine the affect of encapsulation on the sensor, the sensor was characterized before and after encapsulation based on its capacitance change at various frequencies as determined from the VIM. The results presented in Figure 5 shows the sensitivity of the sensor does not change significantly upon encapsulation. The minor offset due to the influence of the silicone coating can be compensated by calibration of each sensor after encapsulation.
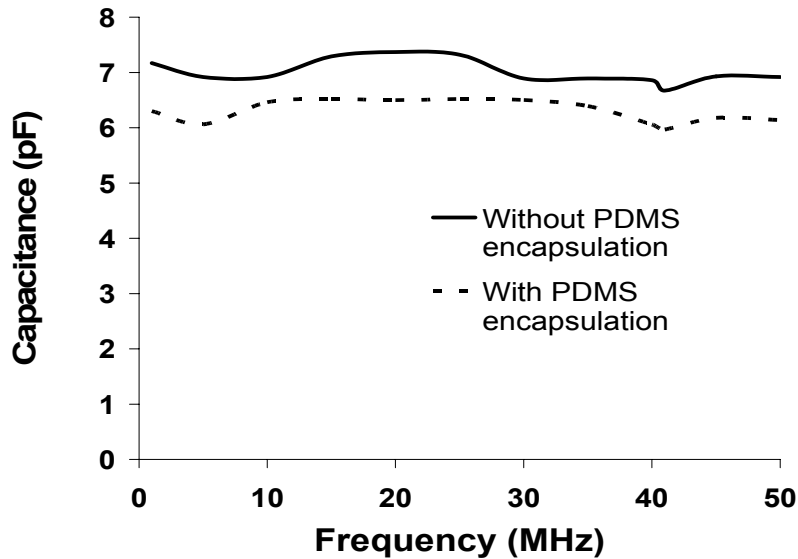

Figure 5: Capacitance change of the pressure sensor relative to change in frequency with and without encapsulation

4.4 Reader antenna performance

To validate the described model by experimentation, four planar reader antennas (Coils A-D) of different sizes, inductance, SRF and number of turns were printed directly onto a PCB. The properties are listed in Table 2. The reader antennas were experimentally evaluated and its performance compared to the theoretical models. The reader antennas were coupled with both the low Q sensor implant and high Q LC resonating circuit consisting of a planar inductor and 22pF chip capacitor. The experimental setup consists of the sensor implant and LC resonant circuit mounted on a vernier calipers and separated from the reader antenna connected to a spectrum analyzer. To determine the maximum read range, the distance between the reader antenna and LC resonant circuit/sensor implant was increased until no further 'dip' in the signal was observed.

Table 2. Antenna coil properties

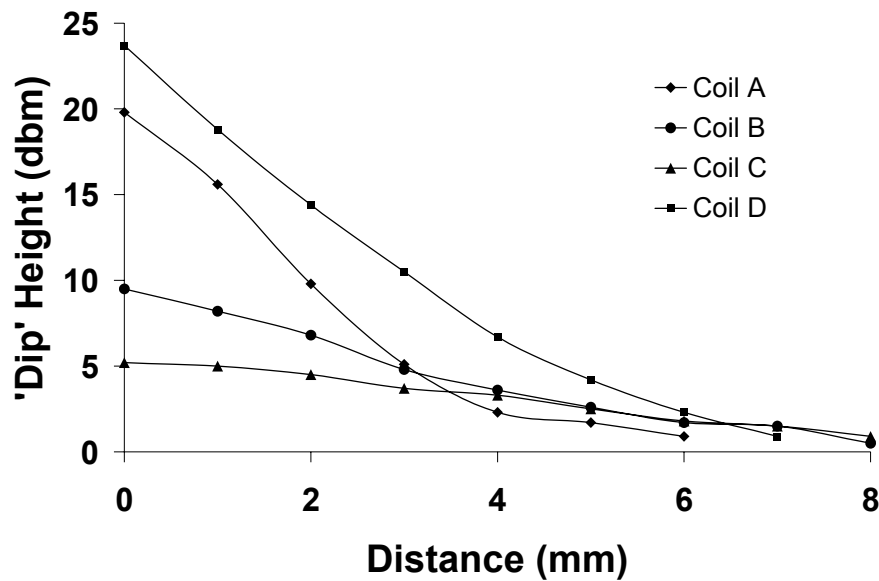|	Coil A	Coil B	Coil C	Coil D
Number of turns	18	15	7	15
Track Width (mm)	0.127	0.254	0.254	0.127
Track Spacing (mm)	0.254	0.762	0.762	0.508
Inductance (μH)	2.14	4.45	2.5	1.75
SRF (MHz)	63	49	73	102
Diameter (mm)	9.4	32.51	32.51	16.76

Figure 6: Evaluation of reader coil geometries at varying distances from the LC resonant circuit. The better coupling results in a greater 'dip' height which decreases with increasing distance from the LC resonating circuit.
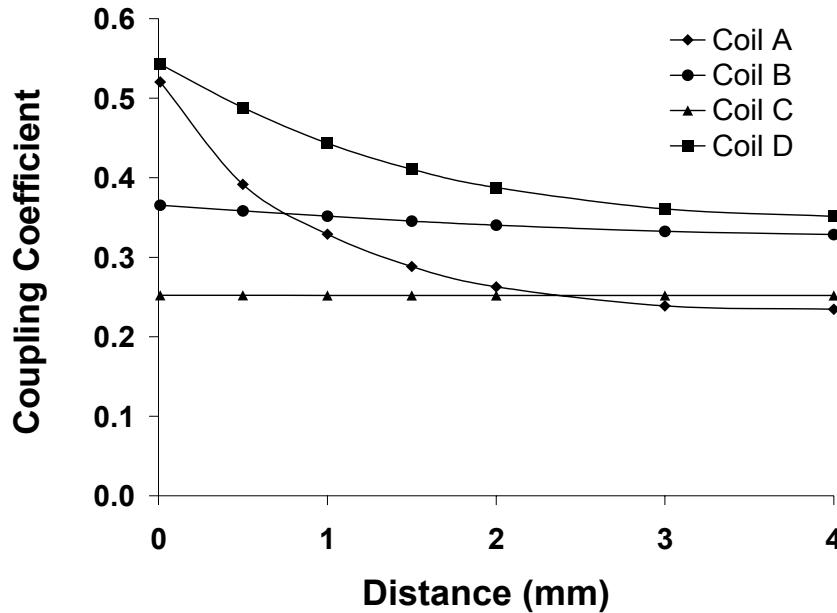
Figure 7: Theoretical coupling coefficients of reader coils at varying distances from the IOP sensor implant calculated from equation (2).

Experimental results showing coupling between the reader antenna and LC resonant circuit represented by the 'dip' height are presented in Figure 6. The theoretical coupling coefficient k between the reader antenna and sensor implant is shown in Figure 7. The theoretical model closely follows the trend from the experimental results (Figure 6).

A summary of results showing the performance of each reader coil with the LC resonant circuit and sensor implant are presented in Table 3. The maximum read range between the reader antenna and sensor implant is affected due to the low Q of the sensor implant as compared to a high Q LC resonant circuit. Experimental results as seen in Figure 6 show that both coil B & C have a maximum read range of 8 mm, with coil B showing greater coupling due to the larger number of turns. Coil A, identical to the sensor inductor has a greater coupling than coil B & C at close ranges (< 4mm) with a maximum read range of 6 mm. However, coil A is more sensitive to lateral and angular coil displacements and the signal detected is greatly attenuated as compared with coil B, C & D. An important requirement in the interrogation of any implanted device is that it is not highly sensitive to lateral and angular misalignments. Coil D larger than coil A and smaller than coil B and coil C has the best coupling of all the coils at close range and a maximum read range of 7 mm. The experimental results suggest that equation (6) provides a good approximation to determine the optimal reader antenna size for a specified read range.

Table 3. Summary of results

	Coil A	Coil B	Coil C	Coil D
Theoretical read range (mm) - (6)	4	10	10	6
Experimental range - LC circuit (mm)	6	8	8	7
Experimental range – sensor implant (mm)	3	0	0	4

4.5 Effect of self resonating frequency

The effect of SRF on the reader coil performance is evident when coupled with the sensor implant. The SRF is the frequency beyond which the inductor starts to behave as a capacitor. Although coil B gives a maximum read range of 8 mm with the LC resonant circuit it produces zero 'dip' when coupled with the sensor implant. This is due to a) low Q of the sensor implant, b) the SRF of coil B is in close proximity to the resonant frequency of the sensor implant. Thus the reader coil should be designed such that its SRF is at least twice the operating frequency of the resonant circuit of interest.

Coil C was designed such that its SRF (73 MHz) was further away from the resonance frequency of the sensor implant. This was implemented by decreasing its inductance (i.e. reducing the number of turns). However, from equation (5) the M is directly proportional to N on the sensor and reader antenna, hence decreasing N affects the coupling between the reader and sensor antenna as shown by the experimental and theoretical results.

Coil D was designed to overcome the limitations of both coil B and coil C. Its SRF was designed to be roughly twice the operating frequency of the sensor implant (102 MHz) achieved by reducing the size of the coil. The number of turns (N) was maximized to enhance coupling with the sensor implant. It was observed experimentally that coil D gave the maximum read range of 4 mm from the sensor implant. In addition, coil D is larger than the sensor implant and not significantly affected by lateral and angular misalignments. Results suggest that in order to obtain a maximum read range with a low Q resonant circuit a high coupling reader antenna is necessary.

5. CONCLUSION

An IOP sensor implant comprising of a MEMS based capacitive pressure sensor and planar inductor was designed to be incorporated into the explant plate of a Molteno GDI. The IOP sensor implant has been shown to have sufficient resolution to distinguish between normal IOP and glaucomatous condition with excellent reproducibility over time. Better resolution of small differences in IOP will be desirable in future iterations. Pressure chamber tests revealed that sensor sensitivity was not significantly affected by encapsulation with PDMS bio-coating.

The reader antenna is designed to maximize its coupling with the sensor implant. The effects of a low Q sensor implant and SRF of the reader coil on the coupling between the reader and sensor coil have been shown. Theoretical models are proposed to predict the coupling of the reader antenna coils with a resonance circuit of interest including its optimal size for a specified read range. We found the theoretical predictions closely followed experimental results. Signals from the sensor implant were measured though 4 mm thick PDMS barrier and though sheep corneal and scleral tissue indicating high potential for using the system in human subjects.

 The IOP monitoring system incorporated into a glaucoma drainage implant overcomes the design complexity and associated costs of incorporating such a system in an intraocular lens. Such a device will open new perspectives, not only in the management of glaucoma, but also in basic research for mechanisms of glaucoma.

Future work will focus on animal trials to determine the long term stability of the system (i.e. drift). In addition, the MEMS based capacitive sensor can be directly wire bonded onto the PCB rather than using the ceramic packaging (LCC3.0) which will allow space for additional turns of the inductor coil (i.e. reducing the resonance frequency). The effects of variation in atmospheric pressure on the IOP sensor implant need to be further investigated but could be dealt with by a reference device that tracks the ambient atmospheric pressure.

ACKNOWLEDGEMENTS

REFERENCES

[1] Walter P, Schnakenberg U, Vom Bogel G, *et al.* Development of a Completely Encapsulated Intraocular Pressure Sensor [Original Paper]. *Ophthalmic Research* 2000;**32**:278-84.

[2] Schnakenberg. U, Walter. P, Bogel. Gv, *et al.* Initial investigations on systems for measuring intraocular pressure. *Sensors and Actuators* 2000;**85**:287-91.

[3] Eggers T, Draeger J, Hille K, *et al.* Wireless Intra-Ocular Pressure Monitoring System Integrated into an Artificial Lens. *1st Annual International IEEE-EMBS Special Topic Conference on Microtechnologies in Medicine & Biology.* Lyon, France 2000.

[4] Leonardi M, Leunberger P, Bertrand D, Bertsch A, Renaud P. First Steps toward Non-invasive Intraocular Pressure Monitoring with a Sensing Contact Lens. *Investigative Ophthalmology & Visual Science* 2004;**45**:3113-7.

[5] Eysteinsson T, Jonasson F, Sasaki H, *et al.* Central corneal thickness, radius of the corneal curvature and intraocular pressure in normal subjects using non-contact techniques: Reykjavik Eye Study. *Acta Ophthalmol. Scand* 2002;**80**:11-5.

[6] Sajeeda., Kaiser T. Passive Telemetric Readout System. *IEEE Sensors Journal* 2006;**6**:1340-5.

[7] Llobet. A, Gasull. X, Gual A. Understanding Trabecular Meshwork Physiology: A key to the Control of Intraocular Pressure *News in Physiological Sciences* 2003;**18**:205-9.

[8] Ong KG, Grimes CA, Robbins CL, Singh RS. Design and application of a wireless, passive, resonant-circuit environmental monitoring sensor. *Sensors and Actuators* 2001;**A 93**:33-43.

[9] Akar O, Akin T, Najafi K. A wireless batch sealed absolute capacitive pressure sensor. *Sensors and Actuators* 2001;**A95**:29-38.

[10] Zierhofer C, M., Hochmair E, S. Geometric Approach for Coupling Enhancement of Magnetically Coupled Coils. *IEEE transactions on Biomedical Engineering.* 1996;**43**:708-14.

[11] Reinhold. C, Scholz. P, John. W, Hilleringmann. U. Efficient Antenna Design of Inductive Coupled RFID-Systems with High Power Demand. *Journal of Communications* 2007;**2**:14-23.